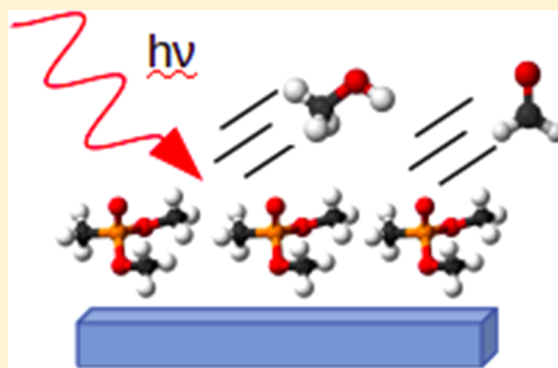


Fate of Some Chemical Warfare Simulants Adsorbed on an Inert Surface when Exposed to Rapid Laser Initiated Heating

K. D. Gibson and S. J. Sibener*

The James Franck Institute and Department of Chemistry The University of Chicago, 929 E. 57th Street, Chicago, Illinois 60637, United States

ABSTRACT: The pyrolysis products resulting from the rapid laser heating of low concentrations of adsorbed chemical warfare simulants have been examined. Specifically, three GB simulants were reacted in this manner: dimethyl methylphosphonate (DMMP), diethyl ethyl phosphonate, and diisopropyl methylphosphonate (DIMP) as well as one HD simulant: 2-chloroethyl ethyl sulfide (CEES). A cryogenically cooled and chemically inert sapphire surface, held in a vacuum chamber, was dosed with a molecular beam of the simulant, and a pulsed CO₂ transversely excited atmospheric laser was used to induce rapid temperature jumps. The coverage of simulant attained between laser pulses was never more than 10%. The plume of reacted and desorbed gases was then analyzed by a combination of time-of-flight measurements and mass spectrometry. We were able to vary the apparent surface temperature between ~600 and ~2400 K. The least reactive simulant was CEES, where ~70% was desorbed as the parent molecule without reaction. The branching ratio between reaction and desorption increased for increasing large R–O groups, with 10% of the DMMP unreacted at 2300 K, but almost all of the DIMP decomposed at ~1200 K. These fundamental measurements on the pyrolysis chemistry of these four molecules shed new, quantitative insights into their thermal chemistry and likelihood of their decomposition when subjected to controlled rates of rapid heating to reach elevated temperatures.



INTRODUCTION

In this paper, we report on the pyrolysis and desorption of some chemical warfare agent (CWA) simulants upon rapid heating. There have been studies of decomposition on catalytic surfaces, such as metals,^{1–4} TiO₂ and Y₂O₃,^{5–9} and supported catalysts.^{10,11} In this paper, we used a more inert surface, which was held in a vacuum, where the only reaction is largely due to heating. This is a contemporary topic for the chemistry community, given the need to understand the efficacy of various destruction and mitigation processes for such chemicals. Moreover, incineration is used to destroy CWA stockpiles, and pyrolysis may be a source of unwanted emissions when the incinerator is either malfunctioning or achieving incomplete decomposition.¹² Pyrolysis of CWAs can also be important when there is a fire or explosion in a contaminated area and there is insufficient O₂ for complete oxidation. Pyrolysis of some selected simulants has been done in gas-phase flow reactors.^{13–16} These experiments involved residence times in the reactor of about 100 ms and involved temperatures of ~700–800 K. These experiments were designed to measure the degradation products and the rates of their formation. We decided to examine the behavior of low concentrations of adsorbed simulants when exposed to rapid heating in the absence of oxygen. The heating was accomplished with a high power IR laser, which rapidly heated the substrate hundreds of degrees in considerably under a millisecond, considering the temporal width of the pulse and

the interaction of high power laser pulses with a photon-adsorbing material.¹⁷ Under these conditions, there are competing pathways: some of the simulants can decompose, but some may be desorbed intact as the parent molecule. The thrust of our experiments was to determine the onset of any simulant degradation as a function of surface temperature. We did not measure all of the possible products, rather our focus was on the crucial fundamental pyrolysis chemistry for these four molecules. This study has shed new, quantitative insights into their thermal chemistry and likelihood of their decomposition or survival when subjected to controlled rates of rapid heating to reach elevated temperatures.

For the experiments described in this paper, we examined four CWA simulants: dimethyl methylphosphonate (DMMP, a GB simulant), diethyl methylphosphonate (DEMP, a GB simulant), diisopropyl methylphosphonate (DIMP, a GB simulant), and 2-chloroethyl ethyl sulfide (CEES, an HD simulant). These simulants were chosen because they have vapor pressures large enough to make a molecular beam. The molecular beam was directed at the surface of cryogenically cooled sapphire, where the simulant was adsorbed. The surface was also exposed to the output of a pulsed CO₂ transversely excited atmospheric (TEA) laser, with the fluence varied so as

Received: June 25, 2018

Revised: September 27, 2018

Published: October 17, 2018

to vary the surface temperature (T_s). Information about the quantity and identity of any molecule leaving the surface was measured using mass spectrometry. The results of these nonequilibrium experiments are that the reactivity varies greatly between simulants, and a great deal of the parent molecule can survive even with high-temperature jumps.

EXPERIMENTAL SECTION

These experiments were done using the Sibener group multiple-molecular-beam gas-surface scattering instrument.¹⁸

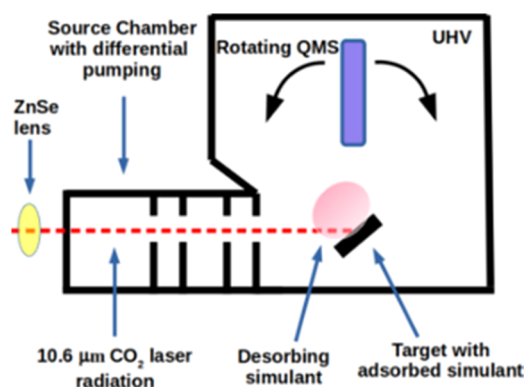


Figure 1. Machine schematic (see text).

A schematic diagram is shown in Figure 1. An Allmark TEA CO₂ laser was used to provide high-fluence pulses for rapid heating (10.6 μm, 4.5–6 J/pulse, roughly Gaussian-shaped temporal profile with a full-width half-maximum of 0.1 ms and an output beam that was 27 × 27 mm²). The IR then impinged upon a ZnSe plano-convex lens with a 1 m focal length mounted on a graduated optical rail. It then entered the low-pressure source region through a ZnSe window. IR continued through the differentially pumped regions of the source chamber and into the ultrahigh vacuum chamber (pressure in the 10⁻⁹ Torr range) where the target was located. Laser fluence could be varied by changing the discharge voltage of the laser or adjusting the lens to target distance. The laser beam spot at the crystal was always much larger in area than the entrance aperture of the highly collimated detector, a doubly differentially pumped quadrupole mass spectrometer (QMS) with an electron impact ionizer. The detector angle relative to the surface normal was variable, though a relative angle θ of 5° was used for most of the experiments we describe.

The target used was always sapphire, either a 3 mm thick laser window or an 0.5 mm thick crystal with an (0001) face. They were clamped to a tantalum plate that could be cryogenically cooled with liquid nitrogen and resistively heated. The angle relative to the incident beams is variable, but was kept at 45° for these experiments. Sapphire was chosen because it absorbs 10.6 μm radiation, and has a high melting point, 2300 K.¹⁹

Dosing the target was done with a molecular beam that impinged on the surface at a 45° incident angle. The beam was produced using a room-temperature bubbler of the simulant, with 100–150 Torr of Ar as the carrier gas. The expansion was done through a nozzle with a 200 μm pinhole. The vapor pressures of the simulants (0.8 Torr for DMMP,²⁰ 0.4 Torr for DEMP,²⁰ 0.3 Torr for DIMP,²⁰ and 3.4 Torr for CEES²¹) used were just large enough to make this dosing method possible.

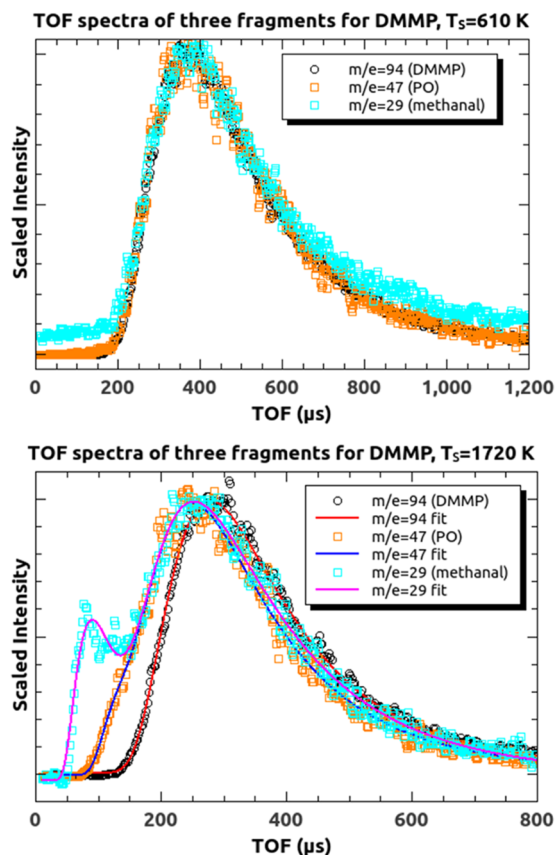


Figure 2. Examples of the TOF spectra for DMMP both below (610 K) and above (1720 K) the surface temperature at which surface reaction occurs. The largest QMS signal for DMMP was $m/e = 94$, $m/e = 47$ would be PO, which could be formed both in the ionizer and due to rapid surface heating. Finally, $m/e = 29$ also shows up in the DMMP QMS signal, but can also be due to formaldehyde formed during the pyrolysis. The two spectra show how the TOF measurements can differentiate between the two events.

The T_a stage had an attached chromel–alumel thermocouple, and dosing was normally done at a surface temperature, T_s , of 120 K. For the sapphire crystal, this was cold enough to grow increasingly thick layers of the simulants with many minutes of dosing, as determined by thermal desorption spectroscopy (TDS), where the surface is slowly heated while measuring the signal of desorbing simulant. Desorption started at 140–150 K. We were unable to deposit any simulant on the sapphire window according to TDS measurements; the thermal conductance to the stage was too low to overcome radiative heating. However, T_s must have been low enough for transient sticking, as we were able to observe pyrolysis products.

The standard procedure set the QMS to pass an m/e of a particular value, expose the target to the simulant beam, pulse the laser at 0.2–1 Hz, and measure the time-of-flight (TOF) signal using a multichannel scaler. The signal was averaged over a number of shots, usually about 50. If more shots were used the signal would decrease, presumably because the sticking coefficient decreased as the surface heated. This was certainly the case with the crystal, as the cooling was not sufficient to keep the stage at 120 K. One laser shot was enough to clean off the surface, so the simulant coverage is whatever adsorbed after a 1–5 s exposure. We do not know what this coverage is, but based on our experience with water

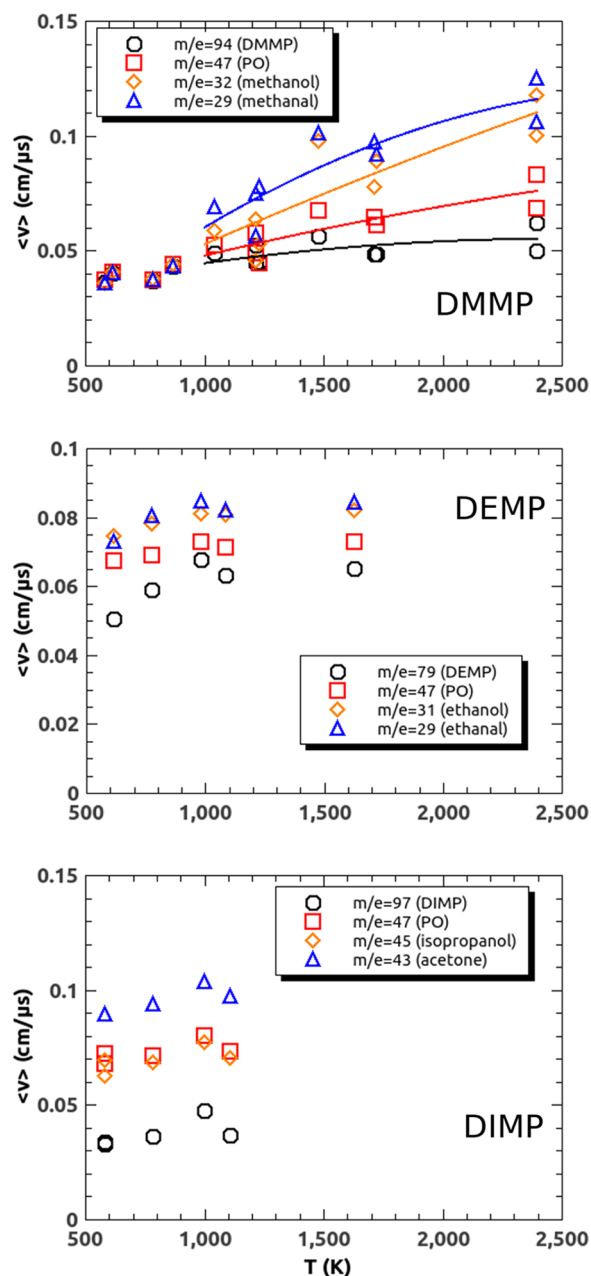


Figure 3. Average velocities for some fragments of the GB simulants from the TOF spectra as a function of surface temperature. The inset indicates the m/e of the fragments and the molecule we speculate may be the surface-produced molecule, which produced that fragment. The lines in the top panel are interpolations meant as guides for the eye.

beams (water has a vapor pressure of 20 Torr at room temperature) this is certainly much less than 10% of a monolayer.

The ionizer electron energy was 100 eV. This produces a large number of fragments in the ionizer for large organic molecules,²² some of which are identical to species formed on the surface. Further, the cracking pattern of molecules can be dependent on the internal energy, as was shown for DMMP,²³ so even a change in relative intensities of the fragments in the mass spectra is not proof of a surface reaction. However, the target to ionizer velocity has to be the same for any fragments produced in the ionizer, but can be much different for reaction

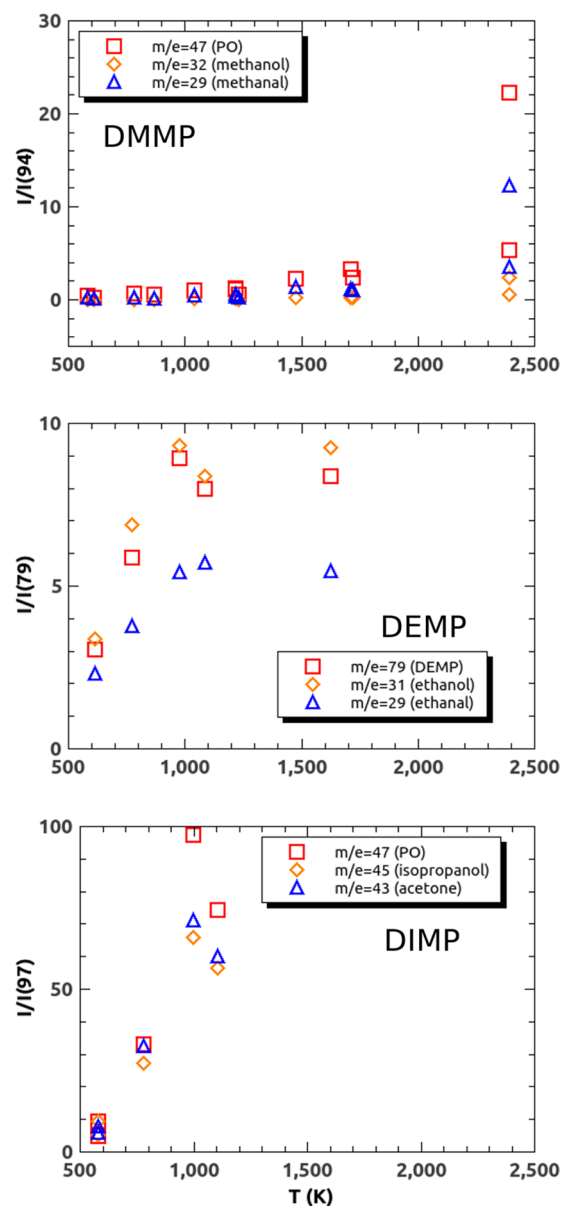


Figure 4. Ratios of the intensities of some fragments of the GB simulants, derived from integrating the TOF spectra, as a function of T_s . The denominator in each case was the most intense fragment from the parent peak of the simulant.

products formed at the surface. An example of this is shown in Figure 2. So, this is our principle indication of pyrolysis. For all of the measurements, we used one of the most intense mass-to-charge (m/e) fragments in the mass spectrum of the molecule, we were expecting.²²

Originally, it was hoped that the translational energy of any desorbed simulant could be used to determine the surface temperature. However, when we measured the angular intensity profile of DMMP, we found it to be much more peaked toward normal than the cosine distribution expected for thermal desorption. So, the temperature was calibrated by using the results for the onset of DMMP pyrolysis from the continuous experiments, 850 K.²³ From the position of the lens, and the measured laser power, we determined the laser fluence. With this number and assuming the temperature was directly proportional to fluence, other temperatures were

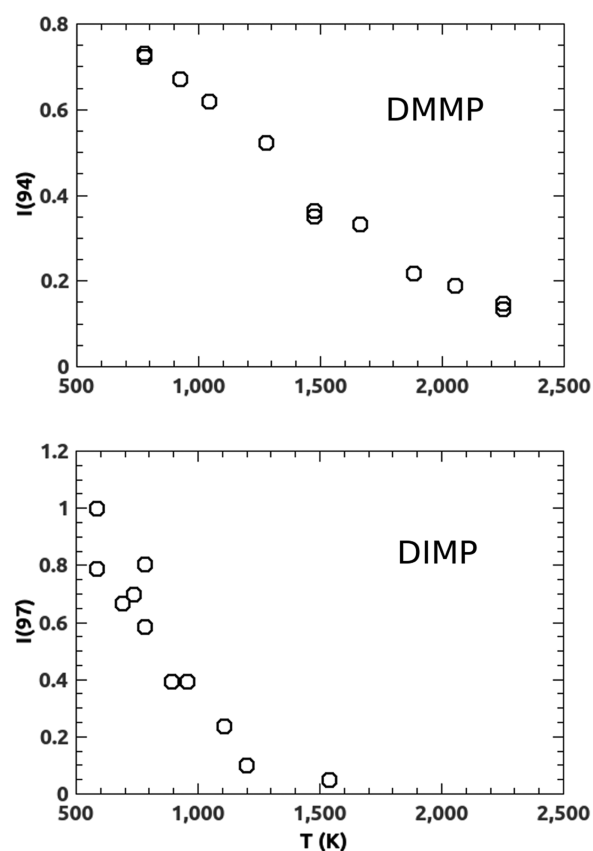


Figure 5. Intensity of the m/e fragment representing DMMP and DIMP as a function of T_s . The incident angle was 45° , and the detector was 5° with respect to the surface normal.

determined by the ratio of the fluence to that where the temperature was estimated to be 850 K. The highest temperatures reached were calculated to be 2300–2400 K, and damage to the polished sapphire surfaces, a slight rippling, was observed. This is consistent to the melting temperature of sapphire, which helps to validate our temperature estimation.

RESULTS AND DISCUSSION

We will first present the results for the GB simulants; DMMP, DEMP, and DIMP. On the basis of quantum chemical calculations,^{24,25} we expected methanol and formaldehyde to be products of the lowest energy pathways of pyrolysis. We also looked for PO ,²⁵ as well as CO and CO_2 , conceivably present because of the oxygen contained in the molecule. For DEMP and DIMP, we looked for the analogous product: an alcohol or aldehyde formed from the side chain. It is important to note that the purpose of this paper is to look at the amount of decomposition versus desorption under conditions of rapid heating. We are not making any definitive statement about the identities of all possible reaction products. For all of these experiments, the laser was pulsed at 0.2 Hz.

Figure 3 shows the velocities of some fragments as a function of T_s . As mentioned, the onset of DMMP decomposition was set at ~ 850 K. Figure 4 shows the intensity ratios of a selected fragment relative to the m/e fragment of the parent molecule with the largest intensity in the mass spectrum. This ratio was taken to correct any day-to-day variations in the dosing beam intensity. Though not shown, we

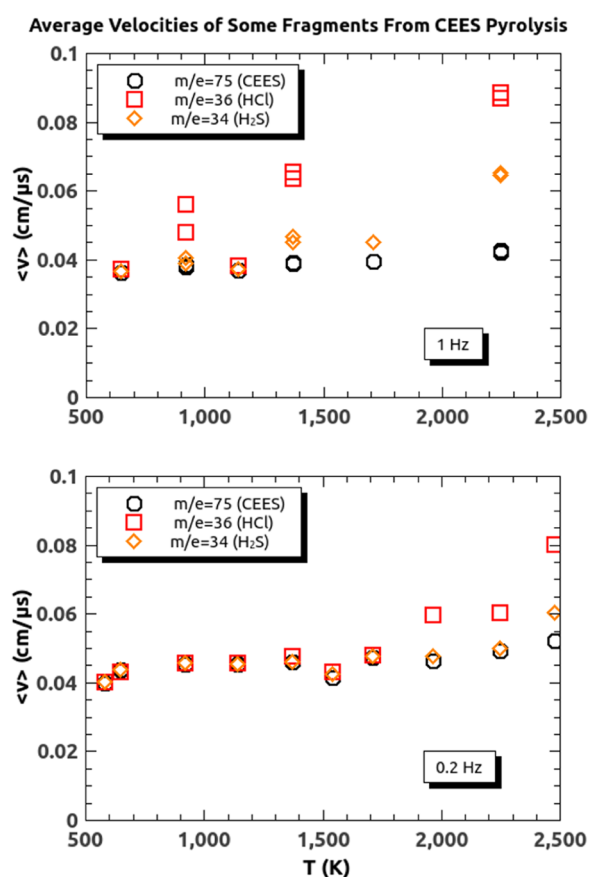


Figure 6. Average velocities for some fragments of the HD simulant CEES from the TOF spectra as a function of surface temperature. The inset indicates the m/e of the fragments and the molecule we speculate may be the surface-produced molecule, which produced that fragment. The inset indicates the frequency of the laser pulses, which is presumably inversely proportional to the relative coverage.

observed the formation of some CO and CO_2 at the higher surface temperatures.

What is apparent is that the amount of pyrolysis seems to be highly dependent on the side chain, with all of the DMMP desorbing intact until T_s is greater than 1500 K, whereas DIMP is largely reacted for T_s well below 1000 K. The difference in the reactivity is clearly shown in Figure 5, where we show the signal due to unreacted simulant.

As mentioned, these experiments had the laser pulsed at 0.2 Hz. If we slowed the rate of laser firing, which allows for more CWA to be adsorbed, eventually we saw little, if any, signal in the TOF spectra, even though post-exposure TDS showed that the surface was free of any simulant. If we dose the surface of the crystal for several minutes to build up a significant overlayer of simulant, and then look for temperature-jump-induced TOF spectra, little, if anything, is observed leaving the surface, even though TDS indicated that all of the simulant were gone. We believe, this behavior indicates that heating is primarily due to the absorption of the IR by the sapphire, so that rapid heating and any reaction take place at the simulant–sapphire interface. The kinetic energy of the products is then dissipated in the simulant overlayer. Presumably, molecules left the surface over a long time period, and possibly less directed toward normal, so that nothing was detected above the background counting rate.

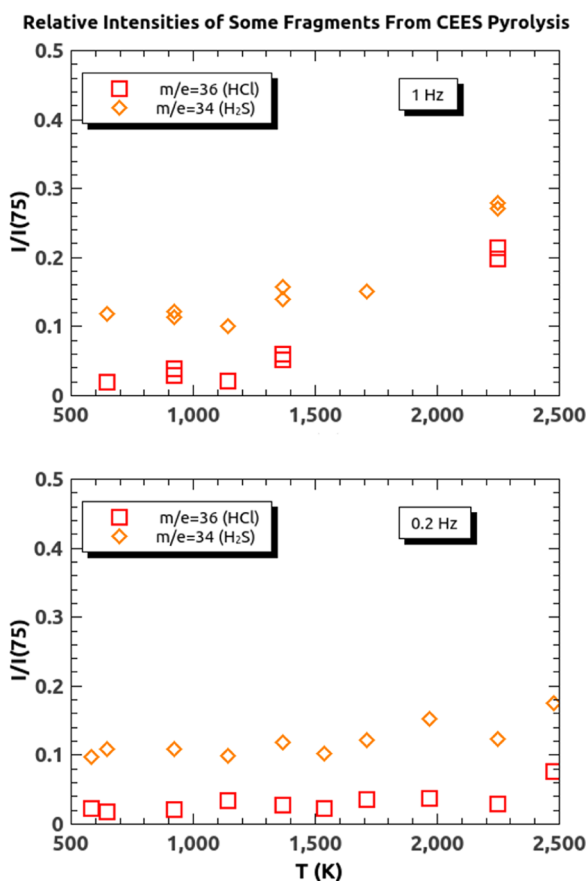


Figure 7. Ratios of the intensities of some fragments of the HD simulant CEES from integrating the TOF spectra as a function of T_s . The denominator in each case was the most intense fragment from the parent peak of the simulant, $m/e = 75$. The inset indicates the frequency of the laser pulses, which is presumably inversely proportional to the relative coverage.

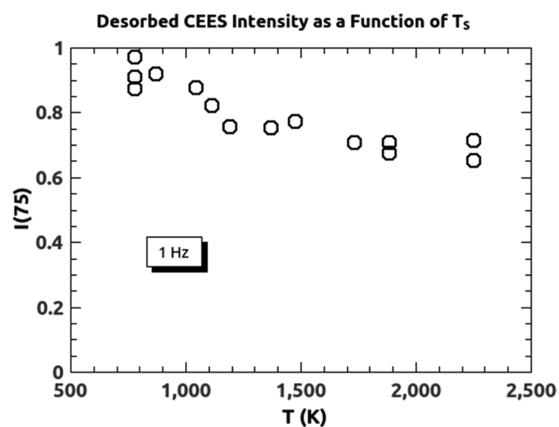


Figure 8. Intensity of the $m/e = 75$ fragment representing CEES as a function of T_s . The incident angle was 45° , and the detector was 5° with respect to the surface normal.

Figure 6 shows the velocities and Figure 7 the intensity ratios for some fragments of CEES pyrolysis. Since CEES had a relatively high vapor pressure (3.4 Torr),²¹ we were able to get reasonable data when pulsing the laser at 1 Hz, since a relatively shorter exposure time still leads to appreciable adsorption with the higher fluence molecular beam. The

figures show the comparison between data taken at 1 and 0.2 Hz. The velocities of the pyrolysis products are significantly higher for the lower surface coverage. Possibly this is due to more collisions in the more dense plume at the higher surface coverage reached, when the laser was only pulsed at 0.2 Hz. The intensity data may show somewhat more pyrolysis at the lower coverage, but Figure 8, where the $m/e = 75$ of the CEES is monitored, shows that there is not much decomposition even at 1 Hz and 2300 K.

CONCLUSIONS

We examined the pyrolysis of low concentrations of surface-adsorbed CWA simulants, three GB simulants (DMMP, DEMP, and DIMP) and the HD simulant, CEES. We continuously dosed a cryogenically cooled sapphire surface with a molecular beam of the simulant and used a pulsed CO_2 TEA laser to induce rapid temperature jumps. The coverage of simulant attained between laser pulses was never more than 10% and probably much less. The plume of reacted and desorbed gases was then analyzed by a combination of time-of-flight velocity analysis and mass spectrometry. We were able to vary the apparent surface temperature between ~ 600 and ~ 2400 K. The least reactive simulant was CEES, where $\sim 70\%$ was desorbed without any reaction. The branching ratio between reaction and desorption increased for increasing large R–O groups, with 10% of the DMMP unreacted at 2300 K, but almost all of the DIMP gone at ~ 1200 K. The important lesson is that under the nonequilibrium conditions of these experiments, the adsorbed molecules may not be fully destroyed, but will be dispersed intact. The degree to which this is true varies with the chosen simulant and experimental conditions. These findings provide new fundamental insights into the thermal chemistry for several molecular simulants that are important for assessing the efficacy of different strategies for destroying such species.

AUTHOR INFORMATION

Corresponding Author

*E-mail: s-sibener@uchicago.edu. Tel.: 773-702-7193.

ORCID

S. J. Sibener: 0000-0002-5298-5484

Notes

The authors declare no competing financial interest.

ACKNOWLEDGMENTS

This work was sponsored by the Defense Threat Reduction Agency (DTRA) under Grant No. HDTRA1-16-1-0024. Additional support was provided by the NSF-Materials Research Science and Engineering Center at The University of Chicago, Grant No. NSF-DMR-14-20709.

REFERENCES

- (1) Ekerdt, J. G.; Klabunde, K. J.; Shapley, J.; White, J.; Yates, J. Surface Chemistry of Organo-Phosphorus Compounds. *J. Phys. Chem.* **1988**, *92*, 6182–6188.
- (2) Hegde, R.; Greenleaf, C.; White, J. Surface-Chemistry of Dimethyl Methylphosphonate on Rh(100). *J. Phys. Chem.* **1985**, *89*, 2886–2891.
- (3) Guo, X.; Yoshinobu, J.; Yates, J. Decomposition of an Organophosphonate Compound (Dimethyl Methylphosphonate) on the Ni(111) and Pd(111) Surfaces. *J. Phys. Chem.* **1990**, *94*, 6839–6842.

- (4) Smentkowski, V.; Hagans, P.; Yates, J. Study of the Catalytic Destruction of Dimethyl Methylphosphonate - Oxidation Over Mo(110). *J. Phys. Chem.* **1988**, *92*, 6351–6357.
- (5) Rusu, C. N.; Yates, J. T. Adsorption and Decomposition of Dimethyl Methylphosphonate on TiO₂. *J. Phys. Chem. B* **2000**, *104*, 12292–12298.
- (6) Panayotov, D. A.; Morris, J. R. Thermal Decomposition of a Chemical Warfare Agent Simulant (DMMP) on TiO₂: Adsorbate Reactions with Lattice Oxygen as Studied by Infrared Spectroscopy. *J. Phys. Chem. C* **2009**, *113*, 15684–15691.
- (7) Ratliff, J. S.; Tenney, S. A.; Hu, X.; Conner, S. F.; Ma, S.; Chen, D. A. Decomposition of Dimethyl Methylphosphonate on Pt, Au, and Au-Pt Clusters Supported on TiO₂(110). *Langmuir* **2009**, *25*, 216–225.
- (8) Gordon, W. O.; Tissue, B. M.; Morris, J. R. Adsorption and Decomposition of Dimethyl Methylphosphonate on Y₂O₃ Nanoparticles. *J. Phys. Chem. C* **2007**, *111*, 3233–3240.
- (9) Panayotov, D. A.; Morris, J. R. Uptake of a Chemical Warfare Agent Simulant (DMMP) on TiO₂: Reactive Adsorption and Active Site Poisoning. *Langmuir* **2009**, *25*, 3652–3658.
- (10) Tesfai, T. M.; Sheinker, V. N.; Mitchell, M. B. Decomposition of Dimethyl Methylphosphonate (DMMP) on Alumina-Supported Iron Oxide. *J. Phys. Chem. B* **1998**, *102*, 7299–7302.
- (11) Panayotov, D. A.; Morris, J. R. Catalytic Degradation of a Chemical Warfare Agent Simulant: Reaction Mechanisms on TiO₂-Supported Au Nanoparticles. *J. Phys. Chem. C* **2008**, *112*, 7496–7502.
- (12) Oppelt, E. T. Incineration Of Hazardous Waste. *JAPCA* **1987**, *37*, 558–586.
- (13) Zegers, E. J. P.; Fisher, E. M. Gas-Phase Pyrolysis of Diisopropyl Methylphosphonate. *Combust. Flame* **1998**, *115*, 230–240.
- (14) Zegers, E. J. P.; Fisher, E. M. Gas-Phase Pyrolysis of Diethyl Methylphosphonate. *Combust. Sci. Technol.* **1996**, *116–117*, 69–89.
- (15) Zheng, X.; Fisher, E. M.; Gouldin, F. C.; Bozzelli, J. W. Pyrolysis and Oxidation of Ethyl Methyl Sulfide in a Flow Reactor. *Combust. Flame* **2011**, *158*, 1049–1058.
- (16) Zheng, X.; Bozzelli, J. W.; Fisher, E. M.; Gouldin, F. C.; Zhu, L. Experimental and Computational Study of Oxidation of Diethyl Sulfide in a Flow Reactor. *Proc. Combust. Inst.* **2011**, *33*, 467–475.
- (17) Ready, J. F. *Effects of High Power Laser Radiation*; Academic Press: New York, 1971.
- (18) Gibson, K. D.; Killelea, D. R.; Yuan, H.; Becker, J. S.; Sibener, S. J. Determination of the Sticking Coefficient and Scattering Dynamics of Water on Ice Using Molecular Beam Techniques. *J. Chem. Phys.* **2011**, *134*, No. 034703.
- (19) Dobrovinskaya, E. R.; Lytvynov, L. A.; Pishchik, V. Properties of Sapphire. In *Sapphire: Material, Manufacturing, Applications*; Pishchik, V., Lytvynov, L. A., Dobrovinskaya, E. R., Eds.; Springer US: Boston, MA, 2009; pp 55–176.
- (20) Butrow, A. B.; Buchanan, J. H.; Tevault, D. E. Vapor Pressure of Organophosphorus Nerve Agent Simulant Compounds. *J. Chem. Eng. Data* **2009**, *54*, 1876–1883.
- (21) Cataldo, D. A.; Ligothke, M. W.; McVeety, B. D.; Bolton, H.; Fellows, R. J.; Li, S.-M. W.; Van Voris, P.; Crecelius, E. A.; Hardy, J. T.; Wentsel, R. S. Acute Environmental Toxicity and Persistence of a Chemical Agent Simulant: 2-Chloroethyl Ethyl Sulfide (CEES). *Chemical Research, Development and Engineering Center*; Defense Technical Information Center, 1988.
- (22) *NIST Chemistry Webbook, NIST Standard Reference Database Number 69*; Linstrom, P. J., Mallard, W. G., Eds.; National Institute of Standards and Technology: Gaithersburg, MD, 2017.
- (23) Gibson, K. D.; Sibener, S. J. Scattering Dynamics, Survival, and Dispersal of Dimethyl Methylphosphonate Interacting with the Surface of Multilayer Graphene. *J. Phys. Chem. A* **2016**, *120*, 4863–4871.
- (24) Yang, L.; Shroll, R. M.; Zhang, J.; Lourderaj, U.; Hase, W. L. Theoretical Investigation of Mechanisms for the Gas-Phase Unimolecular Decomposition of DMMP. *J. Phys. Chem. A* **2009**, *113*, 13762–13771.
- (25) Liang, S.; Hemberger, P.; Neisius, N. M.; Bodi, A.; Gruetzmacher, H.; Levalois-Gruetzmacher, J.; Gaan, S. Elucidating the Thermal Decomposition of Dimethyl Methylphosphonate by Vacuum Ultraviolet (VUV) Photoionization: Pathways to the PO Radical, a Key Species in Flame-Retardant Mechanisms. *Chem. - Eur. J.* **2015**, *21*, 1073–1080.